Giulio Russo, Tobias Unkauf, Doris Meier, Esther Veronika Wenzel, Nora Langreder, Kai-Thomas Schneider, Rebecca Wiesner, Ralf Bischoff, Volker Stadler and Stefan Dübel*

In vitro evolution of *myc*-tag antibodies: in-depth specificity and affinity analysis of Myc1-9E10 and Hyper-Myc

https://doi.org/10.1515/hsz-2021-0405
Received November 1, 2021; accepted February 28, 2022; published online March 22, 2022

Abstract: One of the most widely used epitope tags is the myc-tag, recognized by the anti-c-Myc hybridoma antibody Myc1-9E10. Combining error-prone PCR, DNA shuffling and phage display, we generated an anti-c-Myc antibody variant (Hyper-Myc) with monovalent affinity improved to 18 nM and thermal stability increased by 37%. Quantification of capillary immunoblots and by flow cytometry demonstrated improved antigen detection by Hyper-Myc. Further, three different species variants of this antibody were generated to allow the use of either anti-human, anti-mouse or anti-rabbit Fc secondary antibodies for detection. We characterized the specificity of both antibodies in depth: individual amino acid exchange mapping demonstrated that the recognized epitope was not changed by the *in vitro* evolution process. A laser printed array of 29,127 different epitopes representing all human linear B-cell epitopes of the Immune Epitope Database allowing to chart unwanted reactivities with mimotopes showed these to be very low for both antibodies and not increased for Hyper-Myc despite its improved affinity. The very low background reactivity of Hyper-Myc was confirmed by staining of myc-tag transgenic zebrafish whole mounts. Hyper-Myc retains the very high specificity of Myc1-9E10 while allowing myc-tag detection at lower concentrations and with either anti-mouse, anti-rabbit or anti human secondary antibodies.

Keywords: epitope mapping; hypermyc; myc-tag; peptide microarrays; phage display; recombinant antibody.

Introduction

Epitope tags allow for generic detection of transgenic proteins

Reverse genetics approaches using gene overexpression, dominant negative, and transgene expression *in vitro* and *in vivo*, opened new ways to assess wild type and mutant gene functions. Heterologous gene expression studies typically rely on the availability of a sensitive and specific transgene detection system. Epitope tagging of transgenic proteins allows for specific yet generic detection by adding DNA encoding a short peptide to the open reading frame of the transgene. This peptide contains the linear epitope of an anti-tag antibody. Jarvik and Telmer already in 1998 listed 17 different epitope tags with length between 6 and 15 amino acids (Jarvik and Telmer 1998) that could be fused to the C- or N-term of the protein, but they can also be placed within the gene sequence, located in a loop or other accessible regions where no negative impact on the folding and functionality is induced (Shanbaky and Pressley 1994).

Tagging transgene products with a generic epitope avoids the effort and problems of using transgene protein-specific antibodies. Even if such an antibody is available from a catalogue, its reactivity in the particular assay

Giulio Russo and Tobias Unkauf have contributed equally to this work.

***Corresponding author: Stefan Dübel**, Department of Biotechnology, Technische Universität Braunschweig, Spielmannstr. 7, D-38106 Braunschweig, Germany, E-mail: s.duebel@tu-bs.de. https://orcid.org/0000-0001-8811-7390
Giulio Russo and Esther Veronika Wenzel, Department of Biotechnology, Technische Universität Braunschweig, Spielmannstr. 7, D-38106 Braunschweig, Germany; and Abcalis GmbH, Inhoffenstr. 7, D-38124 Braunschweig, Germany. https://orcid.org/0000-0003-4099-6968 (G. Russo)
Tobias Unkauf, Doris Meier and Kai-Thomas Schneider, Department of Biotechnology, Technische Universität Braunschweig, Spielmannstr. 7, D-38106 Braunschweig, Germany
Nora Langreder, Department of Biotechnology, Technische Universität Braunschweig, Spielmannstr. 7, D-38106 Braunschweig, Germany; and iTUBS mbH, Wilhelmsgarten 3, D-38100 Braunschweig, Germany
Rebecca Wiesner, Technische Universität Braunschweig, Institut für Medizinische und Pharmazeutische Chemie, Beethovenstr. 55, D-38106 Braunschweig, Germany
Ralf Bischoff, Division of Functional Genome Analysis, Research Program "Functional and Structural Genomics", German Cancer Research Center, Im Neuenheimer Feld 280, D-69120 Heidelberg, Germany
Volker Stadler, Pepperprint GmbH, Rischerstrasse 12, D-69123 Heidelberg, Germany

needed is not assured: monoclonal antibodies are often not capable of recognizing the protein both in its native conformation as well in denatured form, while the polyclonal antisera often cause unwanted secondary reactions (Berglund et al. 2008; Bradbury and Plückthun 2015; Goodman 2018; Taussig et al. 2018). Epitope tagging is not only used to detect the protein of interest, but can also be used for protein–protein interaction studies (Fujiwara et al. 2002), protein pull-downs (Ng et al. 1993), and protein purification (e.g. strep-tag) (Schmidt and Skerra 1993). Frequently used tags include the 8 aa FLAG tag (DYKDDDDK), a synthetic peptide; the 9 aa HA tag (YPYDVPDYA) derived from Human influenza virus hemagglutinin, or the synthetic six histidine tag which is also useful for affinity chromatographic purification of the tagged protein (Jarvik and Telmer 1998).

The c-Myc-tag antibody Myc1-9E10

One of the most commonly used epitope tags is the myc-tag containing the core epitope EQKLISEEDL (myc-epitope or myc-peptide). Myc-tag (also named c-Myc-tag, myc-tag or cmyc-tag) is typically detected by the monoclonal antibody Myc1-9E10 (in many publications abbreviated as "9E10") (Evan et al. 1985), as indicated by >8000 citations on CiteAb (www.citeab.com) and >33,000 hits in Google Scholar. This mouse IgG producing hybridoma was raised against a synthetic peptide corresponding to residues 408 through 432 of the 62 kDa human nuclear oncoprotein myc (c-Myc), which it can bind only in its denatured form, relying on a linear and continuous epitope.

The c-Myc epitope peptide has been employed as a tag for different recombinant fusion proteins expressed *in vitro* and *in vivo* in a vast spectrum of applications. Recombinant single chain fragment variable (scFv) antibodies expressed in *Escherichia coli* or mammalian cells were C-terminally tagged for detection in ELISA (Dübel et al. 1993; Ward et al. 1989), Western blot (Ward et al. 1989) flow cytometry, and immunohistochemistry (Kleymann et al. 1995). This epitope tagging system also allowed to immunoprecipitate the *Xenopus laevis* Na,K-pump beta3 recombinant subunits fused to myc-epitope (Gloor et al. 1995), or to trace the vesicular transport processes from the Golgi to the plasma membrane in yeast cells (TerBush and Novick 1995), among countless other applications.

Co-crystallization of the Myc1-9E10 Fab fragment in complex with the myc-epitope (Krauss et al. 2008), unveiled the presence of an atypical interaction. CDR H1 and CDR H3 of the antibody form a cleft to fit the peptide. Interestingly, CDR H3 is unusually extended (18 aa) and uses its "back side" to interact with the peptide, almost like a protruding finger. Epitope substitution analysis helped to define the exact epitope-paratope interface of interaction (Hilpert et al. 2001). Nevertheless, the contribution of neighboring amino acids to the peptide epitope detection has only recently been assessed (Schüchner et al. 2020). In this work, Schüchner and colleagues showed for N-terminal tagged proteins that the fusion of different amino acids to the carboxyterminal side of the myc-peptide (EQKLISEEDLXXXX) can impact Myc1-9E10 binding more than other anti-c-Myc mAbs that bind closer to the N-terminal of the epitope tag. Particularly, Myc1-9E10 binding to the peptide EQKLISEEDLLRKR, when fused to the N-terminal of a protein, resulted in a 20 times higher signal compared to the EQKLISEEDLNGST peptide.

The Myc1-9E10 VH and VL sequences (Fuchs et al. 1997; Schiweck et al. 1997) were initially cloned since the hybridoma showed some problems in cultivation. As it was not easy to produce the scFv version in *E. coli*, it was mutated to generate the derivative 3DX that could be more efficiently expressed and showed increased affinity (from 80 to 23 nM and thermal stability (from 52 °C to 58 °C) (Fujiwara et al. 2002). In this study, we describe further improvements resulting in full IgG derivatives of Myc1-9E10 with increased affinity and thermal stability, but uncompromised specificity. Further, variants of this antibody were generated to be compatible with anti-human or anti-rabbit Fc detection systems. Peptide array-based epitope scanning studies provided new insights into the single epitope amino acid contribution to the binding compared to previous studies (Hilpert et al. 2001). These findings also account for the known peculiarity of the Myc1-9E10-myc peptide interaction (Krauss et al. 2008; Schüchner et al. 2020).

Results

In vitro evolution of anti-c-Myc antibodies

Starting from the Myc1-9E10 derived 3DX scFv gene (Fujiwara et al. 2002), an antibody gene library for antibody selection via phage display was generated by error prone PCR as previously described (Wong et al. 2006). For this specific purpose, the mutated scFv genes were cloned into the myc-tag-free antibody phage display vector pHAL47 derived from pHAL30 (Kügler et al. 2015). The resulting library consisted of 5×10^7 independent clones, with an insert rate higher than 85%.

This library was used to isolate specific binders on immobilized myc-peptide by phage display panning

(Frenzel et al. 2017) for specific binders on immobilized myc-peptide. Panning was performed as previously described (Russo et al. 2018a). A high hit-rate of 79.8% (n = 92) was observed as expected since the library was derived from an already functional scFv antibody gene.

The 21 recombinant monoclonal scFv antibodies with the highest signal to noise ratio (indicating higher producibility and/or higher affinity), were selected from the positive hits and subcloned into the pCSE2.6-hIgG-Fc-XP mammalian expression vector (Jäger et al. 2013) to provide fusion to a human IgG1-Fc. These constructs were used to transfect HEK293-6E cells for transient production of bivalent scFv-Fc fusions, followed by Protein A affinity chromatography purification from the supernatant.

Microscale Thermophoresis (MST) was used to determine the affinity of the antibody-antigen interaction in equilibrium using dye-conjugated myc-peptide. Some antibodies with slightly improved affinities were identified (Figure 1, for raw data see Supplementary Table 1). In addition, a thermal stability ranking was made by determination of the scFv-Fc melting temperatures (T_M) with differential scanning fluorimetry (DSF) (Supplementary Figure 1). The results indicate that antibodies with improved thermostability were generated (Figure 1, for raw data see Supplementary Table 1).

Ten antibodies that showed superior thermal stability and/or affinity compared to the parental 3DX clone and that contained unique mutations (TUN142-4A4, TUN154-4F9, TUN154-8G7, TUN154-8E9, TUN154-12B1, TUN154-12B5, TUN154-12C4, TUN154-12C5, TUN154-12D12 and TUN154-12G1) were used for the construction of a DNA shuffling library. A library consisting of 8×10^7 independent clones was generated. Since the minimal diversity necessary to cover every possible combination of these mutations would be 2.3×10^6, this library provided complete coverage of the maximal possible diversity with 40-fold redundancy.

To get an insight of the actual library diversity, the sequences from 30 randomly picked clones were analyzed (Supplementary Figure 2). Despite the small number of sequences analyzed, it was possible to find almost all (21/22) of the input mutations present in the ten clones used to construct the DNA shuffling library. Furthermore, the parental 3DX clone gene – that was not used as an input sequence – was also found among the 30 analyzed clones, indicating efficient DNA shuffling. Panning of the DNA shuffling library was performed on myc-peptide coated MTPs. The antibody panning campaign resulted in the discovery of 23 novel antibodies. Compared to the input clones – bearing 2.2 mutations in average – DNA shuffled

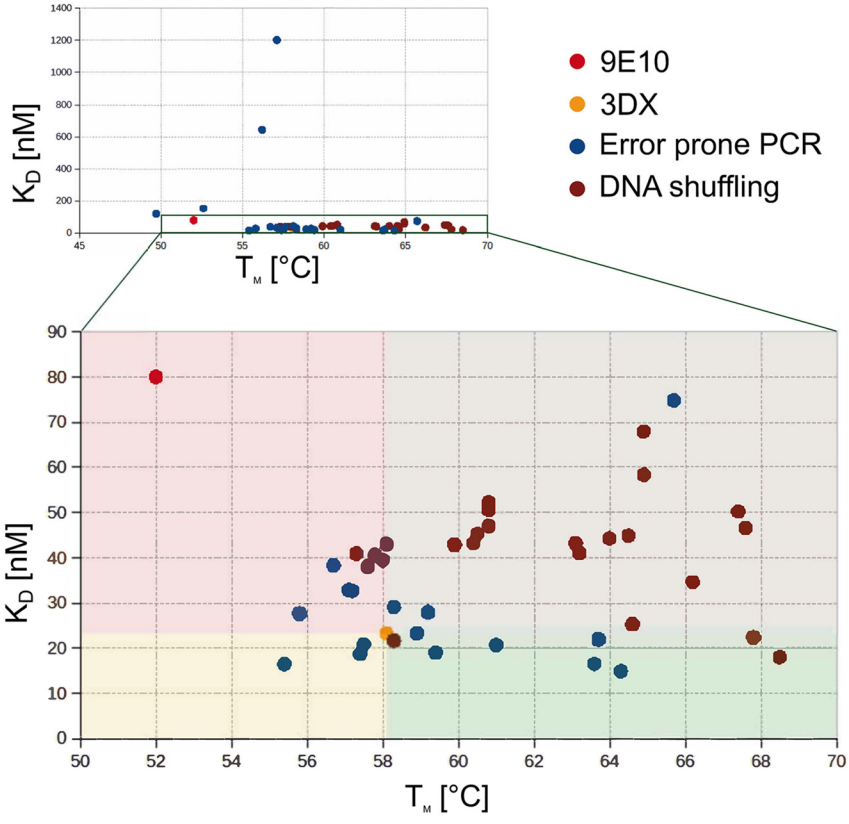

Figure 1: Scatter-plot of affinity versus thermal stability for each of the generated antibodies.
The four colored gates help visualizing the antibody clone properties in comparison to 3DX (orange dot). The green gate shows clones with both better thermal stability and higher affinity. TUN219-2C1 (Hyper-Myc).

clones contained 3.2 mutations in average. DNA shuffling phage display derived antibody genes were produced as fusions to the human Fc, and their thermal stability profile and bivalent affinity were determined as described (Figure 1, for raw data see Supplementary Table 2).

Table 1 compares the success rate of the *in vitro* evolution process expressed as percentage of antibodies with improved features over the parental clone 3DX. Of the total 44 scFv-Fc antibodies studied in MST and DSF (Figure 1), 13.7% showed thermal stability comparable ($T_M \pm 0.5$ °C) to the parental 3DX clone, 27.3% antibodies showed reduced stability, while the remaining 59% showed improved thermal stability. The most thermostable antibody (TUN219-2C1) showed an increase in T_M of 10 °C. Affinity measured using MST revealed that 25% of the new antibody clones showed improved binding compared to the parental 3DX antibody, and 93.2% showed higher affinity compared to Myc1-9E10. Interestingly, 72.7% of the clones that showed lower K_D than 3DX were derived from the error prone library, also 69.2% of the clones with improved thermal stability originated from the DNA shuffling library. This suggests that the error-prone PCR approach has been successful to discover mutations that led to increased affinity (38.1%) as well as thermal stability of the antibody (38.1%), while the following DNA shuffling approach mainly boosted the thermal stability (78.3%), but not anymore the affinity (13.0%). Nevertheless, it was the combination of the two approaches that produced a clone, named Hyper-Myc, with slightly improved affinity and dramatically increased temperature stability.

To maintain the excellent specificity profile of Myc1-9E10, thermal stability is an important factor because it has been shown that somatic mutations that reduce protein stability by increasing conformational dynamics correlate with an increase in binding promiscuity (Dimitrov et al. 2014). Comparing the results of studies conducted at protein level with the analysis of the corresponding antibody amino acidic sequence (Supplementary Figure 2), it is possible to trace back the contribution of each mutation in modifying specific phenotypical protein features. P14S, G128D, G135S, G136V, A151T, P186S mutations have been found in the sequence of antibodies showing slightly increased affinity compared to the parental clone, but similar temperature stability. Intriguingly, none of these mutations where also found in the tested bivalent antibodies showing increased affinity as well as T_M. Among these mutations, only G136V occurred with high frequency in the library (6/30 randomly sequenced clones). One other mutation that occurred with comparable frequency is A23V. A characterized clone carrying only this mutation, TUN154-12G1, showed an affinity decrease of 221% over the parental clone, while an increase in T_M of 55%. Since the phage display antibody selection was based on binding strength to the antigen and producibility as soluble scFv, but not on temperature screening, one could speculate that mutation A23V confers an advantage over other clones in respect of antibody-phage producibility in *E. coli*, which would lead to the over-representation of the clone after antibody-phage amplification. Beside this exception, all other mutations that occurred with high frequency are all conferring improved binding over the parental clone. These mutations, H59Q, H59Y, P61S, and P61R are concentrated in a mutational hot-spot. The only three clones that showed higher affinity as well as higher T_M are all carrying, among others, a mutation in position 59, 61 or both. Particularly, the best error-prone derived clone, TUN154-12C4, contains mutations H59Y, P61S, and G129D. After DNA shuffling and antibody stability ranking, the mutation P61S/R could be found in all ten antibodies showing the highest thermal stability, while H59Q/Y was present in four out of ten. Interestingly, the four most stable clones also carried mutation A121T which was present in only one of the clones selected as input for the generation of the DNA-shuffling library.

The average affinity of the best ten antibodies derived from DNA-shuffling was 31.7 nM. Interestingly, this value does not exceed the average affinity of the ten clones generated via error prone PCR used for the generation of the DNA shuffling library (25.2 nM). Since DNA-shuffling derived clones have an average mutation rate of 3.2, compared to 2.2 of the error-prone PCR derived clones, it is interesting that the combination of different affinity improving mutations did not generate any further affinity increase. This phenomenon may be due to the presence of a structural affinity limit at around 15 nM (Figure 1) intrinsic to this particular paratope-epitope interface. In contrast, thermal stability improved by combination of multiple

Table 1: Percentage of clones showing more than 0.5× units increase or decrease in measured melting temperatures (T_M) or affinity compared to parental 3DX antibody.

Affinity	Error-prone PCR		DNA-shuffling	
>Parental clone	38.1 %	(8/21)	13.0 %	(3/23)
≃Parental clone	4.8 %	(1/21)	0.0 %	(0/23)
<Parental clone	57.1 %	(12/21)	87.0 %	(20/23)
Thermal stability	**Error-prone PCR**		**DNA-shuffling**	
>Parental clone	38.1 %	(8/21)	78.3 %	(18/23)
≃Parental clone	9.5 %	(2/21)	13.0 %	(3/23)
<Parental clone	52.4 %	(11/21)	8.7 %	(2/23)

The testing included 21 scFv-Fc antibodies selected from error-prone PCR phage display library and 23 from the DNA-shuffling library.

stabilizing mutations that were previously discovered via error-prone PCR. The ten most stable antibodies originating from DNA-shuffling have an average T_M of 66 °C, while those from error-prone PCR only 61 °C.

Fine specificity and cross reactivity

To assess the fine specificity, a three-step strategy was chosen. First, the minimal epitope region was identified on epitope arrays. Here, the sequence of human Myc proto-oncogene protein (UniProt ID P01106) was covered by 15-mers having 14 amino acids overlap reciprocally, for a total of 439 different peptides. These peptides were arranged in duplicate for the generation of a high resolution PEPperMAP® Epitope Mapping microarray with 878 peptide spots, further framed by 82 HA (YPYDVPDYAG) positive control peptides. Hyper-Myc and Myc1-9E10 showed an identical core epitope region recognition: EQK**LISEEDL** (Figure 2A), defined as the epitope region the which absence completely abolishes binding. From this assay, the contribution of N-terminal QK could not be evaluated in detail. For both Myc1-9E10 and TUN219-2C1, a very weak second response against peptides with the consensus motif KLVSE was observed. The latter two aspects were addressed in the following Epitope Substitution Scan.

To assess whether the fine specificity for the myc-peptide was not compromised by the *in vitro* evolution process, the role of every individual amino acid position within the epitope region was assessed by generating arrays with complete random amino acid exchanges at every position. For this purpose, PEPperMAP® Epitope Substitution Scan arrays of laser printed c-Myc peptide variants were used. This array carries 191 different c-Myc peptide variants since each of the ten amino acid positions of the myc-peptide were exchanged to each of the other 19 main amino acids to determine the substitutions tolerated in each position (Figure 2B). The ratio between the signal intensity obtained from staining a certain peptide variant compared to the original myc-epitope sequence (100% signal), provides the technical means to quantitatively determine the exact degree of sequence conservation per each position. It is evident that the most conserved residues are identical for the two antibodies. The core motif ^{4}LISE^{7} – which is part of the core epitope region ^{4}LISEEDL^{10} – was the most conserved part together with L^{10}, while E^{1} could unambiguously be exchanged. I^{5} only

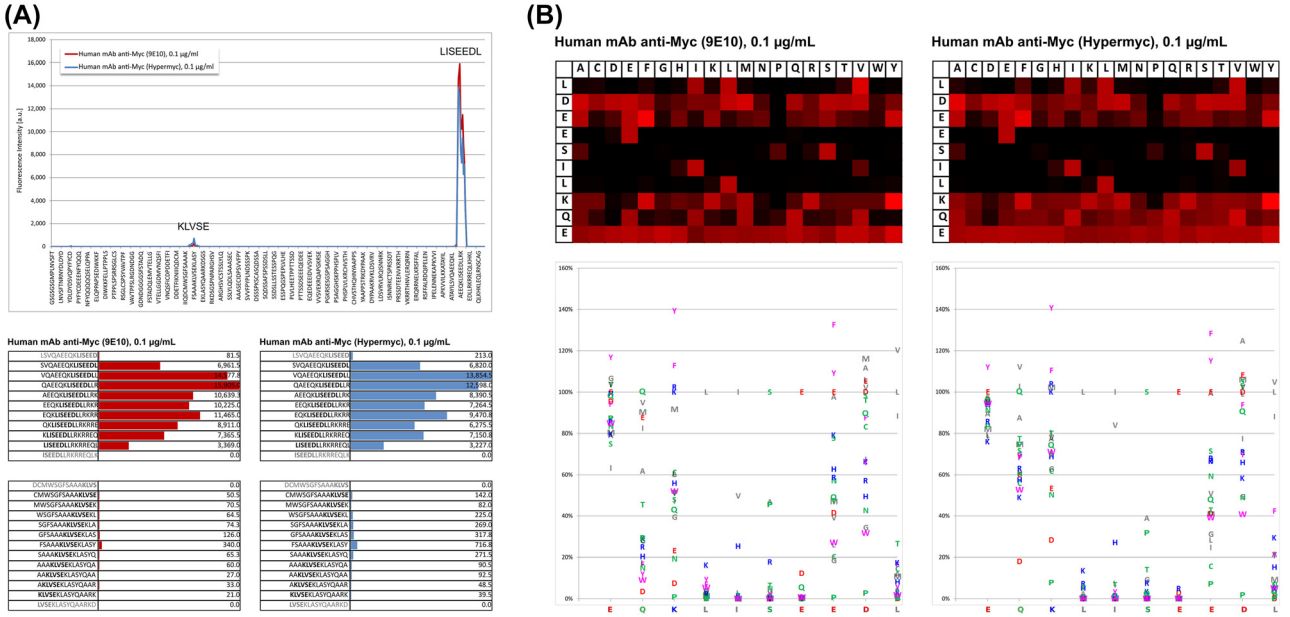

Figure 2: Epitope mapping studies on peptide array.
(A) Hyper-Myc and Myc1-9E10 monoclonal antibodies minimal epitope recognition as determined by PEPperMAP® Epitope Mapping laser printed peptide arrays. Bottom: raw data, top: corresponding intensity plot. Both antibodies showed a primary response towards the consensus motif LISEEDL and a very weak secondary response against the consensus motif KLVSE. (B) PEPperMAP® Epitope Substitution Scans of epitope peptide ^{1}EQKLISEEDL^{10} arrays stained with Myc1-9E10 (left) or Hyper-Myc (right). Top: heat maps corresponding to microarray scan results. Increasing red intensity levels indicate the likelihood that a certain amino acidic substitution is not disrupting the binding, so black indicates substitutions that are not tolerated. Bottom: Position dependent replacement quantification. Binding intensities per each substitution of Myc1-9E10 (left) or Hyper-Myc (right) were normalized to the intensity level obtained with the wild type peptide ^{1}EQKLISEEDL^{10}.

allowed a substitution to V. On the contrary, the residue E^8 – which was found to be part of the core epitope region- could be replaced by nearly any other amino acid but proline without abolishing the binding. Interestingly, some amino acidic substitutions (e.i. K^3Y and E^8F) improved epitope recognition.

Finally, an aspect of specificity as important as the correct recognition of the epitope is the cross-reactivity profile, ideally being the absence of recognition of any other epitopes. A direct approach to check for unwanted cross reactivities is the use of large arrays of antigen structures. Consequently, both Hyper-Myc and Myc1-9E10 were analyzed on 29,127 different epitopes from the human proteome using the PEPperCHIP® Human Epitome Microarray. This peptide microarray represents all human linear B-cell epitopes of the Immune Epitope Database (www.iedb.org/) (Vita et al. 2019) complemented by all epitopes of the most common vaccines. This standard array lacks the wild type myc-epitope. Myc1-9E10 showed only very few and very low signal cross-reactivities (Figure 3). Out of 29,127 tested peptides, only the peptides EEVVGEEKLVSEEIVT and EVQEEGYLAKILVPE showed cross reactivity towards Myc1-9E10 and Hyper-Myc above 10% the signal expected for the binding to the myc-peptide (data not shown). Additionally, only Myc1-9E10 bound the peptide LGITAEDARLVSEIAMH. Overall, these two antibodies cross-reacted with circa 0.007% of the peptides. This low cross-reactivity profile certainly contributed to the broad success of the myc-tag detection system. The differences in terms of cross-reactivity between Myc1-9E10 and Hyper-Myc can be considered as negligible, despite its higher binding affinity to the myc-tag. As to be expected from the epitope mapping array data, this approach also identified a weak cross-reactivity with the LVSE core motif for both antibodies. The collected data also provide a list of potentially cross-reacting human epitopes allowing a bioinformatic check for the occurrence of such motifs in future uses of both Myc1-9E10 and Hyper-Myc.

Flow cytometry

The detection of myc-tagged scFv antibodies in flow cytometry was tested on CD19 positive Daudi cells (human B lymphoblast derived cell line) using an anti CD19 scFv fragment cloned from monoclonal antibody FMC63 that carries a carboxyterminal myc-tag (Figure 4). A concentration dependent increase in binding, represented by the APC signal median, could be shown for both Hyper-Myc and Myc1-9E10 antibody, with the Hyper-Myc resulting in

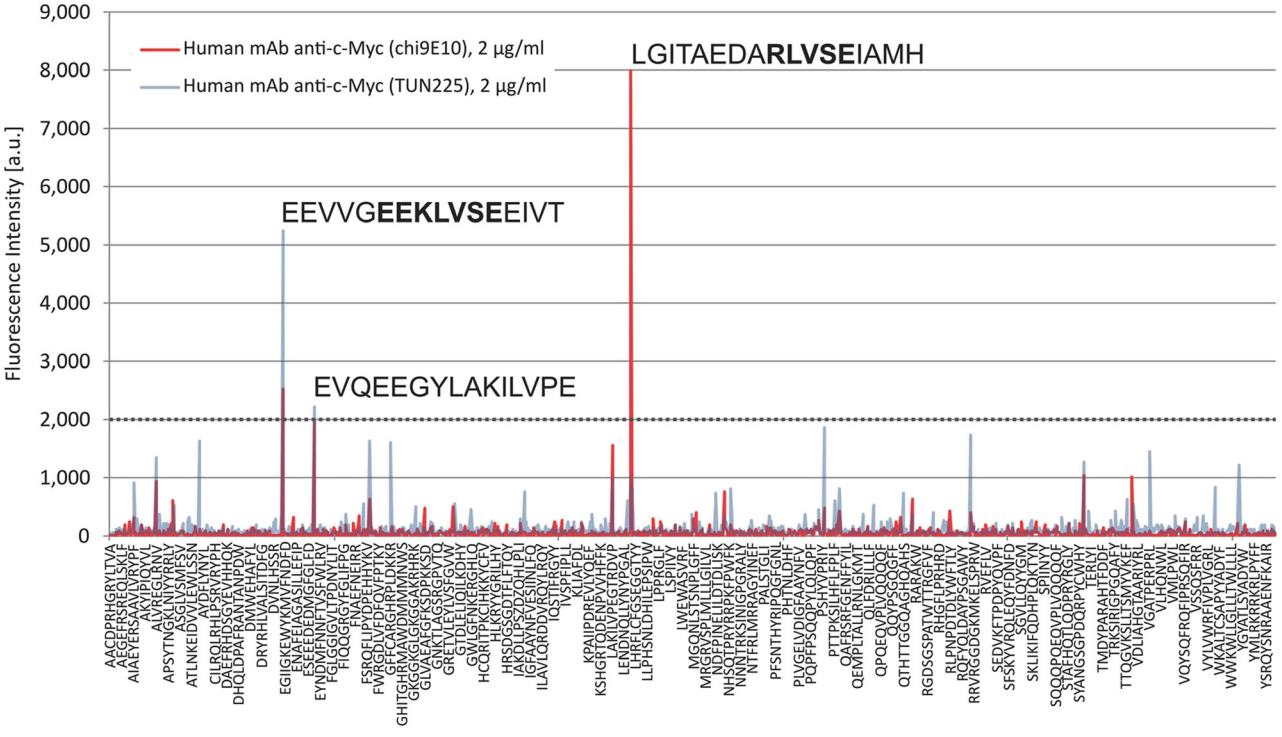

Figure 3: Cross reactivity profiling. Myc1-9E10 (red) or Hyper-Myc (blue) top 1299 peptide hits on PEPperCHIP® Human Epitome Microarray (29,127 human peptides).
A fluorescence signal of 2000 is considered in the range of 10% of the signal generated by antibody incubation on myc-epitope peptide. Myc1-9E10 as well as Hyper-Myc were applied at 2 µg/mL.

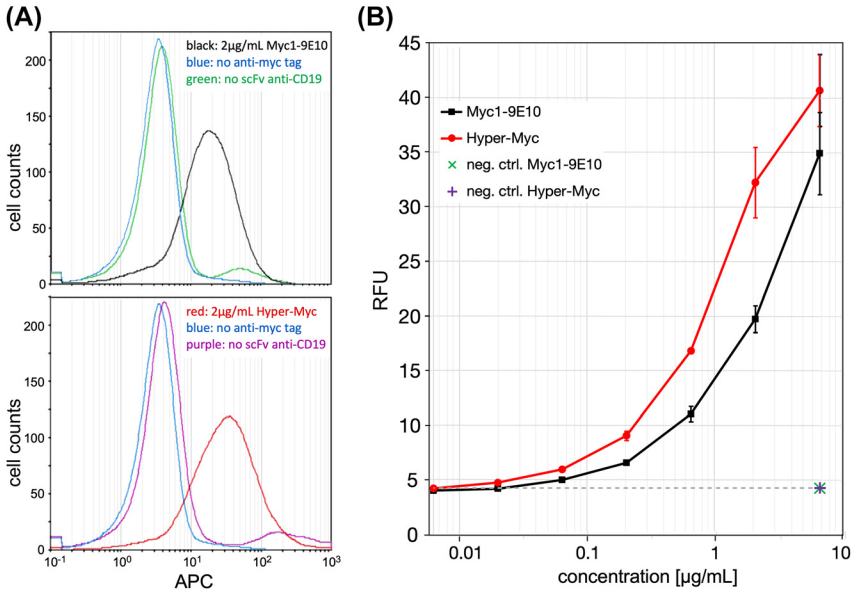

Figure 4: Flow cytometry analysis of myc-tagged antibodies bound to cells.
(A) Histograms of Daudi cells stained with either Myc1-9E10 (top panel) or Hyper-Myc (bottom panel) in the presence or absence of primary anti-CD19 scFv myc-tagged antibody fragment. Histograms are shown for concentrations of 2 µg/mL of Myc1-9E10 or Hyper-Myc, or 6.32 µg/mL for the negative controls. (B) Sensitivity of detection of myc-tagged anti-CD19 scFv on Daudi cells followed by incubation with either Hyper-Myc (red) or Myc1-9E10 (black) in concentrations ranging from 6.32 ng/mL to 6.32µg/mL. Alive single cells were gated; APC-conjugated goat anti-mouse IgG Fc was used for visualisation, and the median of the APC signal was measured using a MACSQuant flow cytometer. Error bars represent the standard deviation of duplicates.

higher APC signals when applied in the same concentration (Figure 4). Furthermore, no unspecific binding was detected for either the Hyper-Myc or Myc1-9E10 antibody, demonstrating that the increased specific binding of Hyper-Myc did not lead to any increase in background staining, thus matching the observations obtained with the other immunostaining methods.

Whole mount staining of myc-tag-transgenic zebrafish

Whole mounts of complete organisms contain every protein and other molecule of the entire animal, providing a highly probative milieu to validate antibody specificity. Further, transgenic animal methods allow for knockouts or antigen-reporter fusions of a single protein, providing the ultimate control for immunostainings (Russo et al. 2018b). In this work we used zebrafish (*Danio rerio*) transgenic larvae expressing a myc-peptide C-terminally labelled red fluorescent reporter (mScarlet) under the control of a glial promoter. Thus, transgene expression is restricted to the CNS (Figure 5, red channel). These conditions allow for direct comparison of the anti-c-Myc staining profile versus the fluorescent reporter expression pattern. Two days post fertilization mScarlet-myc positive zebrafish larvae were fixed in 4% FA and used for staining with mouse Hyper-Myc or Myc1-9E10 antibodies at 0.1 µg/mL concentration (Figure 5, green channel). The transparency of the zebrafish larvae allows to acquire fluorescent signal from the stained larvae and define the degree of the fluorescent signal overlap (Figure 5, merge). Hyper-Myc and Myc1-9E10 antibodies could both detect the fluorescent protein C-terminally fused to myc-tag, but with slight differences in specificity and sensitivity. Hyper-Myc staining fully matched the mScarlet-myc expression pattern and did not stain any additional tissues. In contrast, while the same amount of Myc1-9E10 also provided a very low background staining, it failed to visualize all of the mScarlet positive tissue, indicating a recognizably lower sensitivity. Furthermore, in the 'merge' picture, it can be noticed that Myc1-9E10, but not Hyper-Myc, weakly stained the outer surface of the mScarlet-myc negative larvae, while no such background staining is observed when using anti-mouse Alexa-488 conjugated secondary antibody alone.

Immunoblots and capillary electrophoresis-based immunoassay (CEIA)

In immunoblots of myc-tagged proteins spiked into cell lysates, both Myc1-9E10 and Hyper-Myc stained a single

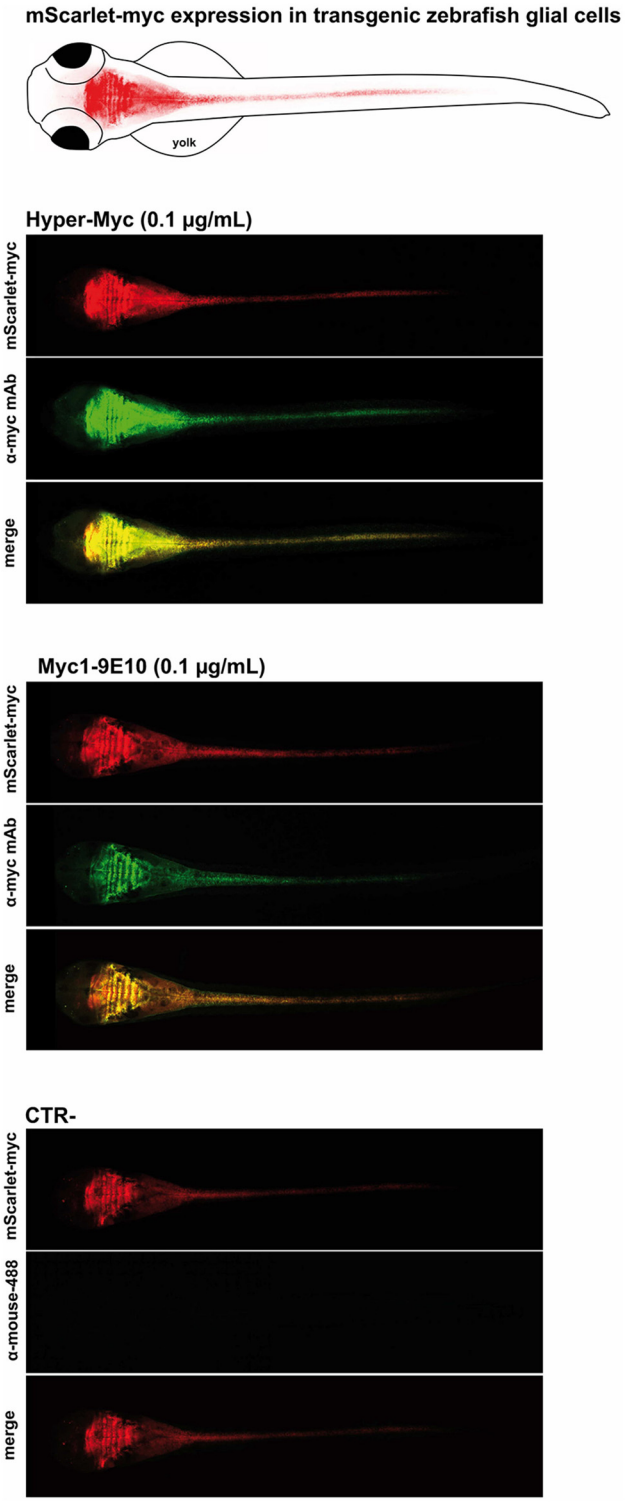

Figure 5: Whole mount immunofluorescence analysis of 2dpf mScarlet-myc positive transgenic zebrafish using Hyper-Myc (top), Myc1-9E10 (middle), or secondary antibody control (bottom). The myc-epitope is expressed as C-terminal fusion tag at the red fluorescent reporter mScarlet.

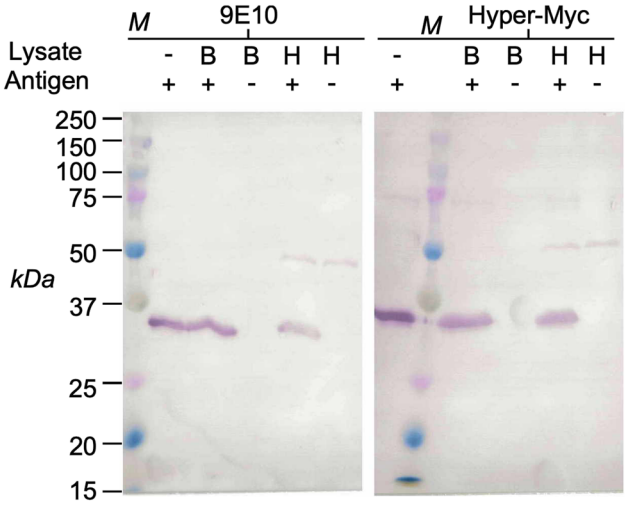

Figure 6: Immunoblots of cell lysates containing 100 ng per lane of a myc-tagged scFv fragment.
B, *E.coli* total cell lysate, H, human cells (Expi293F cell line), M, marker.

band with the expected molecular mass (Figure 6). All faint additional bands visible on the blots can be attributed to antigen or lysate reactions with the secondary antibody.

Simple Western ImmunoassayTM (WES) (ProteinSimple, a Bio-Techne Brand, San Jose, CA, USA) is an automated capillary immunoblot technology that allows the exact quantitation of immunostaining after capillary electrophoresis SDS (CE-SDS). A recombinant C-terminally myc-tagged antigen of 42 kDa was detected using mouse IgG Hyper-Myc or Myc1-9E10. Anti-mouse HRP-conjugated antibody was used for detection and visualization with chemiluminescent substrate. The electropherogram (Figure 7) allowed for quantification within a broad dynamic range of primary antibody concentrations. Hyper-Myc showed improved binding, e.g. almost doubled the signal at 2 µg/mL. The computer-generated (Western blot-like) view visualizes the higher sensitivity of the Hyper-Myc, in accordance with its higher affinity.

Stability and antigen binding of rabbit, human and mouse Hyper-Myc

The antibody clone TUN219-2C1 showed the highest T_M (68.5 °C) and one of the lowest K_D (18 nm). The VH and VL encoding gene fragments of this antibody were subcloned into mammalian expression vectors in frame with DNA encoding an N-terminal signal peptide and C-terminal human IgG1, mouse IgG2a, or rabbit IgG heavy and kappa

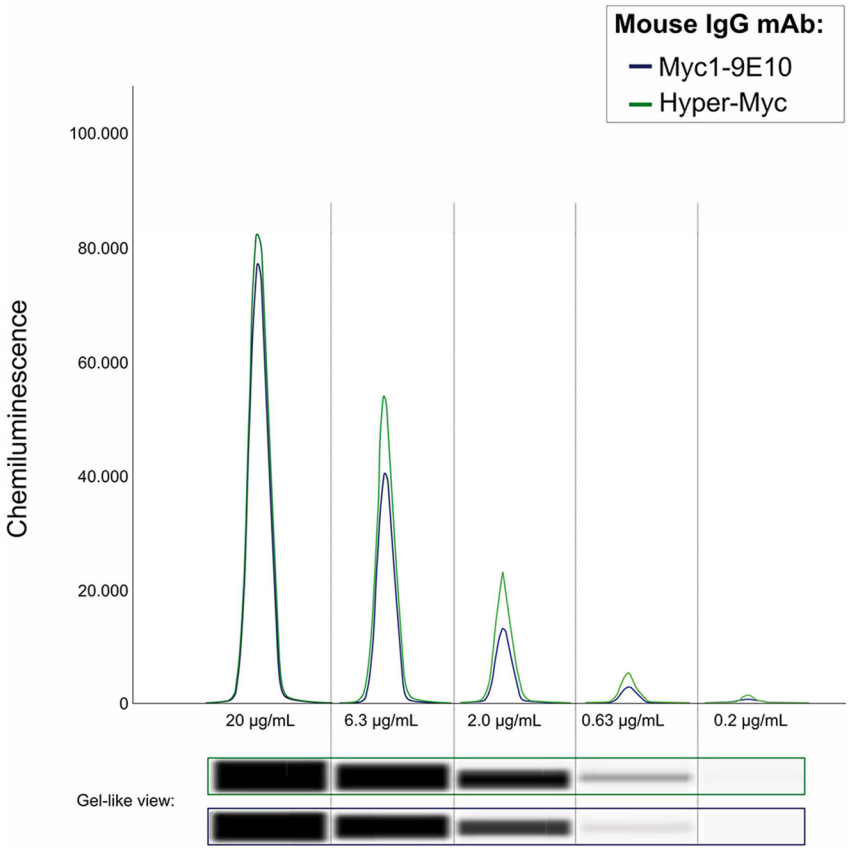

Figure 7: Quantitative immunodetection of myc-peptide labelled antigen with mouse IgG Hyper-Myc or Myc1-9E10 using the automated Protein Simple™ Western Immunoassay system. Electropherograms represent quantitative chemiluminescence signal per each tested antibody concentration. Bottom: automatically generated gel-like data illustration.

light chain genes respectively. Combination of heavy and light chain vectors were used for transient production in suspension cells of whole IgG molecules. After Protein A column affinity purification, IgG antibody purity and quality were assessed via size exclusion chromatography (SEC). Rabbit, human and mouse kappa IgG variants of TUN219-2C1 showed comparable profile in SEC with close to 100% of the molecule present in the monomeric fraction due to the absence of aggregates, dimers or breakdown products (Figure 8A). Binding to myc-peptide was verified in ELISA on plate immobilized myc-peptide labelled unrelated protein (Figure 8B).

Since thermal stability has been shown to not strongly correlate with shelf-life (Wang and Roberts 2013), long term storage of the Hyper-Myc IgG was analyzed by storage in solution at 4 °C in the absence of any stabilizer or preservative for more than 6 months. No significant loss of binding activity in ELISA was detected for any of the three Hyper-Myc species variants (Figure 8B), with EC_{50} values (in nM) of 1.02 versus 1.02 (Myc1-9E10), 0.86 versus 1.24 (Hyper-Myc with mIgG2a-Fc), 0.73 versus 0.84 (Hyper-Myc with hIgG1-Fc) or 0.30 versus 0.31 (Hyper-Myc with rbIgG-Fc) for the fresh versus 7 month/4 °C storage sample, respectively. Absolute signal values in indirect ELISA can strongly influenced by the necessity to use different secondary antibodies, hence it is not possible to directly compare EC_{50} of the different species IgG formats using these results.

Discussion

In the past years, a growing number of publications identified substantial problems with the quality of many of today's research antibodies (Baker 2015; Bradbury and Plückthun 2015; Goodman 2018). While a large fraction of these problems result from the use of polyclonal antisera, also limitations of the hybridoma method were reported. A multicentric sequencing study found that more than 30% of 185 randomly picked hybridomas expressed additional productive antibody chains (Bradbury et al. 2018). This not only reduced sensitivity in direct comparison to the corresponding recombinant monoclonal antibody by diluting the "correct" IgG with unwanted byproducts, but also compromised specificity. Since the supernatant of hybridoma cells expressing more than one light chain contains a mix of three different IgG species, these antibodies do not provide the quality a user expects from a "monoclonal"

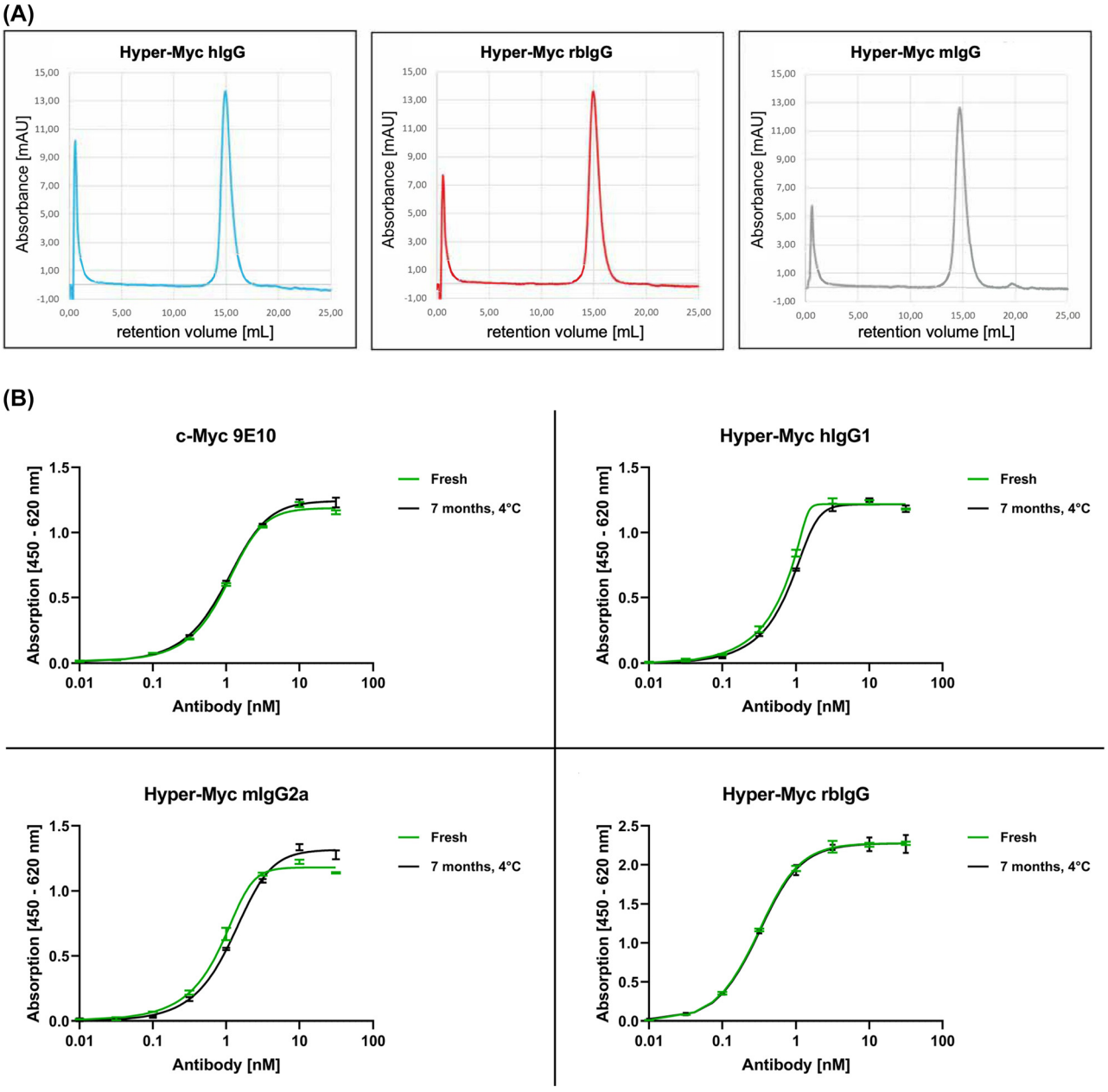

Figure 8: Antibody stability assessment.
(A) Size exclusion chromatography (SEC) analysis of different Hyper-Myc IgG variants with constant parts of human IgG1 (left panel), rabbit IgG (middle panel) or mouse IgG2a (right panel). (B) Shelf-life of Myc1-9E10 hybridoma antibody was compared to the three different versions of Hyper-Myc. Each antibody was stored for a period of seven months at 4 °C prior testing in triplicate in ELISA. An aliquot stored at −80 °C for the same period of time was freshly thawed and used as reference. The aliquots did not contain any protectants nor stabilizers. Error bars represent the standard deviation. Asymmetric Sigmoidal, five parameter logistic (5 PL) curve fitting was used to determine the EC_{50} values.

reagent. Finally, the storage of hybridoma cell lines in liquid nitrogen is costly. Hence, hybridoma antibodies sequencing and conversion to a recombinant format of choice is becoming a widely used approach to improve product continuity and eliminating the need and the risk of storying the clones in liquid nitrogen. A report recently published by the European Union even recommends to exclusively use recombinant antibodies in the future (Gray et al. 2020; Halder et al. 2020).

In addition to the higher quality and reproducibility expected from antibodies that are defined by their primary sequence, *in vitro* evolution techniques can be adopted to

further improve the antibody functional and biophysical properties. In this work we successfully used phage display to select affinity and particularly thermal stability improved variants of the Myc1-9E10-derived 3DX antibody after *in vitro* evolution. The best clone resulting from this *in vitro* optimization, Hyper-Myc, performed favorably in multiple assays against Myc1-9E10 in a head-to-head comparison, demonstrating improved sensitivity without loss of specificity, most significantly, without a compromised cross-reactivity profile despite the higher affinity.

The latter is evident from the combined results of the three epitope analysis assays that allowed to establish a very detailed specificity profile of the analyzed antibodies. The myc-tag residues involved in the binding to Myc1-9E10 are unchanged for Hyper-Myc: not only the core epitope region ^{4}LISEEDL^{10} (Figure 2A) is identical between the two antibodies, also the residues where substitutions are not tolerated are identical. Consisting with these results, the epitope substitution analysis showed that the ^{4}LISE^{7} plus L^{10} is the main interaction motif with the antibody paratope as only few to zero substitutions in these positions could be tolerated. These results are in accordance to a previous work by Hilpert and colleagues from 2001 (Hilpert et al. 2001), which identifies ^{4}LISE^{7} as core binding motif and identified ^{3}KLISEED^{10} as the minimum epitope region of Myc1-9E10. Nevertheless, in their work using pep-spot membrane epitope substitution matrixes, Hilpert at al. found that L^{10} substitutions are tolerated depending on the presence or absence of a C-terminally fused Asparagine. This phenomenon is also described by Schüchner and colleagues (Schüchner et al. 2020), who reported variations in Myc1-9E10 signal strength when detecting myc-tag fused to different neighboring residues.

The binding to myc-peptide is retained when the isoleucine in position 5 is replaced with a valine (LISE –> LVSE). This explains why the two tested antibodies showed slight secondary reaction towards the motif KLVSE/LVSE in the human B-cell Epitope microarray. This example shows that the identification of permissive substitutions can be used to predict real cross reactivities.

Overall, only two minor differences could be identified between Myc1-9E10 and Hyper-Myc in the panel of tolerated amino acidic substitutions. Myc1-9E10 was shown to tolerate Q2E substitution better than Hyper-Myc, *vice versa* for I5V substitution. Not surprisingly, both antibodies slightly cross-reacted to the peptide EEVVGEEKLVSEEIVT, containing the motif ^{1}EEKLVSEEIV^{10} (Figure 3). The cross-reactivity was 2 times higher for Hyper-Myc, hence the higher tolerance to I5V substitution could have had a higher impact than Q2E in the arising of this minor cross-reactivity. On the other hand, the cross-reactivity to LGITAEDARLVSEIAMH peptide, also containing the LVSE motif, was 8 times higher for Myc1-9E10. Here, the result is in contrast with the higher tolerance of Hyper-Myc towards I5V mutation. This shows that changes in the overall epitope structure and charge may have a more significant impact on the binding than single amino acidic substitution. For example, the portion of hydrophobic/acid residues in the myc-tag (30%/40%) is quite different from those of the cross-reactive peptide (52.94%/17.65%).

As the specificity profile of Hyper-Myc was not found to be compromised, Hyper-Myc, allowed to obtain higher sensitivity and without increase of background staining. This has been demonstrated so far for whole mount immunofluorescence, flow cytometry and immunoblots, while a similar increased sensitivity can be expected in other immunoassays as well. This of course always requires careful assessment of any cross-reactivity when using different tissues or other methods, since antigen preservation and epitope accessibility may differ substantially between different assays.

In respect of the changes within the antibody, it was very interesting to observe that no mutations had been identified within the paratope, i.e. the loops contacting the antigen directly. In contrast, all mutations were located in the framework structure, sometimes far away from the

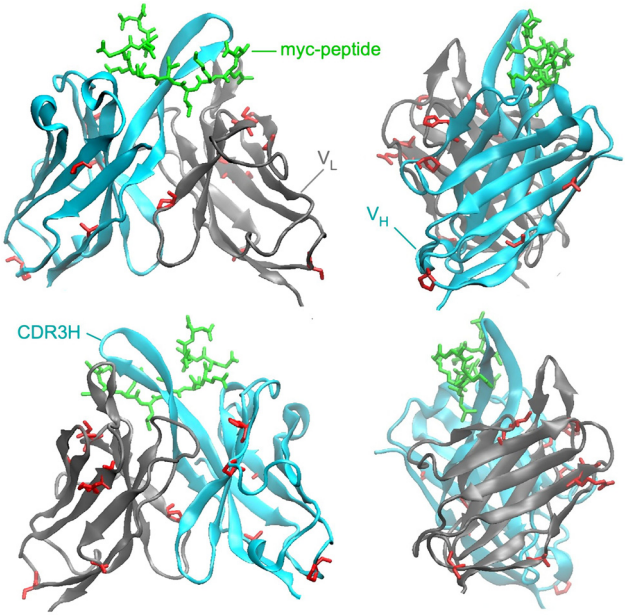

Figure 9: Location of the observed mutations (as listed in Supplementary Figure 2) within the structure of the anti-myc-tag Fv fragment.
The model is based on the crystal structure PDB database no. 2ORB. Amino acid positions where mutations were observed are marked by red side chains. The myc peptide is shown in green.

paratope (Figure 9). This is not unusual if random mutagenesis is applied to affinity maturation, suggesting that the beneficial effects which improved the affinity were more entropic than enthalpic. Significantly, several mutations were found in the scFv Gly-Ser linker peptide initially (G128D, G129D, G135S, G136Vm S137Y). However, the conversion to full IgG (without this mutated linker sequences) did not lead to a loss in affinity, indicating that these mutations rather had a positive influence mainly on scFv stability. It would be interesting in the future to analyze these changes in detail by structural analysis as the results may open a way to obtain a new stability improving linker for single chain antibody generation. However, as this could also be a feature linked to the individual antibody sequence used in this study, alternatively, the use of Fab mutagenesis libraries could be exploited to avoid incurring in the risk of selecting for mutations the which impact may be lost in the conversion into IgG format Steinwand et al. (2014).

Recombinant combinations of antigen binding regions of the same antibody with constant regions of immunoglobulins from different species allows to expand the possible combination of primary and secondary antibodies, offering new opportunities to perform double- or triple staining immunoassays (Moutel et al. 2009). Consequently, the choice to use either human, mouse or rabbit secondary antibodies to detect the myc-tag vastly expands its experimental utility, e.g. by facilitating combinations with tens of thousands of mouse monoclonal antibodies in colocalization studies. Another example is the use of the human Fc variant as a standard for human antibody binding, e.g. on peptide arrays.

While the development of Hyper-Myc illustrated how *in vitro* evolution and phage display can be used to immortalize and improve hybridoma antibodies, improvement on the tag itself could be envisaged from the available data. The epitope substitution analysis identified mutations in the myc-tag which seemed to improve epitope recognition (e.i. K3Y and E8F), offering the opportunity to design an affinity improved myc-tag variant. Finally, efficient production of Hyper-Myc can be achieved in serum free medium and thus already fulfills the future requirements of the European Union (Halder et al. 2020) in respect of avoiding animal use in research antibody generation and production. The described *in vitro* evolution method is generally applicable to improve properties like stability and affinity of other anti-tag antibodies, for example to improve the suboptimal affinity of common anti-His6 tag antibodies (Jarvik and Telmer 1998).

Materials and methods

Error-prone PCR and DNA-shuffling antibody gene libraries construction

For the construction of the error-prone PCR library, the 3DX scFv gene (Fujiwara et al. 2002) was amplified using the GeneMorph II Random Mutagenesis Kit (Stratagene) according to manufacturer's instructions. DNA amplification was verified via agarose gel electrophoresis and resulting amplicon band was extracted and purified to serve as template in further mutagenesis rounds. The scFv genes resulting from the third mutagenesis round were cloned into the myc-tag-free pHAL47 antibody phage display vector derived from the more common pHAL30 (Kügler et al. 2015).

DNA shuffling was performed as described by Stemmer and colleagues (Stemmer 1994). In brief, 100 ng of each scFv antibody DNA were aliquoted and digested with DNaseI at 37 °C for different incubation times within 5 and 13 min. From each DNA aliquot, fragments between 100 and 300 bp were further purified and used for primer-free assembly PCR. The resulting material was used as template for shuffled scFv genes amplification and cloning into the pHAL47 vector.

The libraries were packaged with Hyperphage (Rondot et al. 2001; Soltes et al. 2007) for further use in antibody selection in microtiter plate.

Antibody selection in microtiter plate (MTP) and screening ELISA

Hit selection was performed as previously described (Russo et al. 2018a). In brief, 100 ng streptavidin per well were diluted in phosphate buffer saline (PBS) and coated overnight at 4 °C in Costar High binding 96-well plate (Corning, New York, USA). After blocking with 350 µl MPBS-T (2% (w/v) milk powder in PBS; 0.05% Tween20) per well, plates were washed 3 times with PBS-T (PBS; 0.05% Tween20). After washing, 33 ng per well of biotinylated myc-peptide were diluted in PBS and immobilized on streptavidin for 1 h at room temperature (RT). The right amount of phage particles from the library to be used for antibody selection has been set at 100× the estimated library size, calculated in colony forming units (cfu). The libraries were pre-incubated with 150 µl MPBS-T for 1 h to clear them from sticky phage particles. Afterwards, the pre-cleared library was incubated onto the plate-immobilized antigen for 1 h at room temperature. Unbound antibody-phage were removed applying stringent washing conditions repeatedly 30/40/30 times (panning round 1/2/3). Afterwards, the remaining bound phage were eluted by incubation with 10 µg/mL trypsin 30 min at 37 °C and subsequently used for *E. coli* TG1 (OD600 ~0.5) infection in a 96-deep well plate (Greiner Bio-One, Frickenhausen, Germany). The infected culture was incubated for 30 min without and 30 min with shaking (650 rpm) at 37 °C prior the selection of phage infected bacteria by the addition of 1 mL ampicillin-containing medium (2 × YT-GA (1.6% (w/v) Tryptone; 1% (w/v) Yeast extract; 0.5% (w/v) NaCl (pH 7.0); 100 mM D-glucose; 100 µg/mL ampicillin)). After 1 h at 37 °C and 650 rpm, bacterial cells were co-infected with 1×10^{10} cfu M13KO7 helper phage and further incubated for 30 min at 37 °C without and 30 min at 37 °C with shaking.

Afterwards, the culture was centrifugated for 10 min at 3220 g and the resulting supernatant discarded. The bacteria pellet was resuspended in 2 × YT-AK medium (1.6% (w/v) Tryptone; 1% (w/v) yeast extract; 0.5% (w/v) NaCl (pH 7.0); 100 µg/mL ampicillin; 50 µg/mL kanamycin) to select co-infected *E. coli*. Phage amplification was carried out by incubating the co-infected *E. coli* overnight at 30 °C and 650 rpm. Produced antibody-phage particles were separated via centrifugation from the bacterial cells and used for further panning rounds. At the end of the third panning round, phagemid-bearing bacterial cells were plated onto agar plates for the production of soluble monoclonal scFv antibodies and their validation in ELISA. In brief, 150 µL 2 × YT-GA were added to u-shaped 96 well polypropylene plates (U96 PP, Greiner Bio-One) and each well inoculated with a single colony of bacteria bearing scFv expressing phagemids. Plates were incubated overnight at 37 °C and 850 rpm. The following morning, new plates containing 140 µL of fresh 2 × YT-GA medium per well were inoculated with 10 µL solution and incubated at 37 °C and 850 rpm until 0.5 OD600 was reached. Bacteria were pelleted by centrifugation for 10 min at 3220 × *g* and resuspended in 150 µL 2 × YT medium plus 100 µg/mL ampicillin and 50 µM isopropyl-beta D thiogalacto pyranoside (IPTG) prior overnight incubation at 30 °C and 850 rpm. After soluble scFv production, bacteria were harvested by centrifugation for 10 min at 3220 *g* at 4 °C. The scFv production supernatant was transferred into new PP-MTP and used in screening ELISA. For this assay the MTPs were antigen coated and blocked as previously described for the antibody selection procedure. Bacterial supernatant containing monoclonal scFv antibodies was mixed 1:2 with 2% MPBS-T and incubated in the antigen coated plates for 1.5 h at RT followed by three washing steps in PBS-T. Thanks to their C-terminal HIS tag, bound scFv antibodies were detected with mouse anti-hexa-HIS-tag DIA-900 antibody (Dianova, Hamburg, Germany) and goat anti-mouse secondary antibody conjugated to horseradish peroxidase (HRP) (A0168, Sigma). Both antibodies were diluted in 2% MPBS-T. Binding reactions were visualized incubating the HRP substrate tetramethylbenzidine (TMB). The development of the enzymatic reaction was stopped by the addition of 1 N H_2SO_4, then the absorbance was measured in an ELISA plate reader (Epoch, BioTek, Bad Friedrichshall, Germany) at 450 nm using the signal at 620 nm as reference. Positive binders were sequenced and their DNA analyzed using the VBASE2 software (www.vbase2.org) (Mollova et al. 2010).

Antibody cloning and production in the scFv-Fc and IgG formats

Unique scFv antibody genes selected via phage display were subcloned into the pCSE2.6-hIgG1-Fc-XP mammalian expression vector (Jäger et al. 2013) to obtain scFv-hFc antibodies containing the human (h) IgG1-Fc region. The 3DX sequence was synthesized according to Fujiwara et al. (2002). TUN219-2C1 (Hyper-Myc) antibody clone was additionally converted into different species IgG formats by subcloning its VH and VL genes fused to the constant parts of heavy and kappa light chain of human IgG1, mouse IgG2a, and rabbit IgG using the respective variants of the human pCSEH1c (heavy chain) and pCSL3k (light chain kappa) vectors (Steinwand et al. 2014).

Antibodies were produced in mammalian HEK293-6E or EXPI293F cells (Thermo Fisher Scientific) as previously described (Jäger et al. 2013). At 6–7 days post transfection, the cultures were harvested and the secreted antibodies purified via Protein A affinity chromatography as described previously (Jäger et al. 2013). For analytical size exclusion chromatography (SEC), purified Hyper-Myc human, mouse, or rabbit IgG antibodies were run on Superdex 200 Increase 10/300 GL column (Cytiva) according to the manufactures protocol.

Microscale thermophoresis (MST) affinity determination

Antibody affinity towards the myc-peptide was determined in solution by Microscale Thermophoresis (MST) using the Monolith NT. Automated (NanoTemper Technologies GmbH, München, Germany). Fluorescently labelled myc-peptide Atto-647N-x-GGSGGS-EQKLISEEDLNA (Peps4LS GmbH, Heidelberg, Germany) was kept at a concentration of 10 nM while each antibody was serially diluted 1:2 over 12 points starting from a concentration comprised between 0.2 and 1.8 mg/mL. All measurements were performed in duplicate.

Differential scanning fluorimetry (DSF) protein stability determination

Each bivalent scFv-hFc antibody was diluted to a concentration of 40 µg/mL in 25 µL PBS plus 10× Sypro orange. Temperature profiling ranged from 30 °C to 95 °C in 1 °C temperature increase per minute. Fluorescence intensity was acquired at 555 nm upon excitation at 470 nm. All measurements were performed in triplicate.

Peptide arrays, epitope mapping

Peptide arrays were produced by laser-printing (PEPperPRINT GmbH, Germany) according to Stadler et al. (2008). The amino acid sequence of human myc proto-oncogene protein (UniProt ID P01106) was elongated by neutral GSGSGSG linkers at the C- and N-terminus to avoid truncated peptides. The elongated antigen sequence was translated into 15 amino acid peptides with a peptide-peptide overlap of 14 amino acids. The resulting myc-peptide microarrays contained 439 different peptides printed in duplicate (878 peptide spots) and were further framed by additional 82 HA (YPYDVPDYAG) control peptides.

The myc-peptide array was incubated for 15 min in phosphate buffer saline with 0.05% Tween 20 (PBS-T), followed by an initial blocking for 30 min with Rockland Blocking Buffer MB-070 (RBB; Rockland Immunochemicals, USA). After short rinsing with PBS-T, the array was incubated for 16 h at 4 °C with human monoclonal anti-c-Myc (Hyper-Myc) antibody or human monoclonal anti-c-Myc (9E10) antibody at a concentration of 0.1 µg/mL in PBS-T containing 10% RBB. The array was washed three times for 1 min with PBS-T and then incubated for 45 min at room temperature with secondary antibody goat anti-human IgG (H+L) DyLight680 (Rockland Immunochemicals, USA) and with control antibody anti-HA (12CA5) DyLight800 (provided by Dr. G. Moldenhauer, DKFZ) at concentrations of 0.2 µg/ml and 1 µg/mL respectively, in PBS-T containing 10% RBB. Subsequently, the array was washed three times for 1 min with PBS-T and rinsed with 1 mM TRIS, pH 7.4.

After drying of the peptide array, fluorescence images were acquired with an Odyssey Infrared Imager (LICOR, USA) at a resolution of 21 µm. Scanner sensitivity was set to 7.0 for the 700 and 800 nm channels, respectively. The focal plane was set to +0.8 mm. Quantification of spot intensities was based on the 16 bit gray scale tiff files

and microarray image analysis was done with PepSlide® Analyzer (SICASYS Software GmbH, Germany). This software algorithm breaks down fluorescence intensities of each spot into raw, foreground and background signal, and calculates averaged median foreground intensities and spot-to-spot deviations of spot duplicates. Averaged spot intensities of the assays with the sample were plotted against the antigen sequence from the N- to the C-terminus to visualize overall spot intensities and signal-to-noise ratios (intensity plot).

Peptide arrays for epitope substitution scans

Based on wild type myc-epitope EQKLISEEDL, the exchange of all amino acid positions by the 20 main amino acids resulted in substitution scan peptide microarrays with 191 different peptides with a length of 10 amino acids printed in triplicate. The substitution scan peptide microarrays were further framed by 76 additional HA control peptides, and incubated with human Hyper-Myc or human chimeric anti-c-Myc 9E10 (kind gift of Gerd Moldenhauer) at a concentration of 0.1 µg/mL followed by staining with secondary and control antibodies and read-out as described above.

Peptide arrays for cross reactivity profiling

The PEPperCHIP® Human Epitome Microarray (www.pepperprint.com/products/human-epitome-microarray/) covers 29,127 linear peptides printed in duplicate (58,254 peptide spots) as well as additional polio and HA control peptides. The peptide microarray content is based on all linear B-cell epitopes of the Immune Epitope Database (www.iedb.org/) (Vita et al. 2019) with the host "human", and was further complemented by all epitopes of the most common vaccines. Arrays were incubated with human Hyper-Myc antibody or human chimeric anti-c-Myc 9E10 each at a concentration of 2 µg/mL, followed by staining with secondary and control antibodies and read-out as described above.

Immunoblots and capillary electrophoresis-based immunoassay

Immunoblots were done as described (Russo et al. 2018) using 100 ng per lane of the unrelated myc-tagged scFv antibody TM44-C7 in total cell lysates of either *E. coli* or the human cell line Expi293F. Pure antigen or non-spiked cell extracts were used for negative control. Protein A purified Myc1-9E10 or Hyper-Myc (mouse Fc) were used at 1 µg/mL and anti-mouse IgG-AP (Jackson Immunolabs) was used as secondary antibody at 1:30.000.

The WES Simple Western™ capillary electrophoresis-based immunoassay (CEIA) system (ProteinSimple, a Bio-Techne Brand, San Jose, CA, USA) was used for polyacrylamide gel-free and blot-free immunodetection of myc-tag labelled antigen prepared in reducing or denaturing conditions. This quantifiable western blot equivalent system uses small diameter glass capillaries for protein separation and subsequent immobilization to the capillary wall through a UV-activated chemical coupling. Sample preparation, loading and immunodetection was performed in accordance with the manufacturers protocol. A 42 kDa myc-peptide tagged unrelated protein (C-terminal tag fusion) was diluted in DTT containing sample buffer (ProteinSimple, a Bio-Techne Brand, San Jose, CA, USA) to a final concentration of 10 µg/mL. Mouse Hyper-Myc or mouse Myc1-9E10 were serially diluted by the square root of ten starting from an initial concentration of 20 µg/mL until 0.2 µg/mL. Goat anti-mouse HRP-conjugated antibody (A0168, Sigma; 1:300) was used for secondary antibody detection. Chemiluminescent signal was analyzed and plotted using the Compass for Simple Western software (ProteinSimple, a Bio-Techne Brand, San Jose, CA, USA).

Flow cytometry

For comparison of Hyper-Myc and Myc1-9E10 antibody in flow cytometry 5×10^5 Daudi cells (CD19+, ATCC) were washed with FACS buffer (2% FCS, 5 mM EDTA in 1× PBS) and subsequently centrifuged for 4 min at 280 *g* and 4 °C. Cells were resuspended in 8 µg/mL myc-tagged anti-CD19 scFv (clone FMC63, GenBank: MN702884.1) and incubated for 45 min on ice. The cells were washed again prior to applying either Hyper-Myc or Myc1-9E10 antibody with concentrations ranging from 6.32 ng/mL to 6.32 µg/mL. For background control, only the highest concentration of 6.32 µg/mL was used. Cells were incubated another 45 min on ice and washed again. Staining was performed using APC-conjugated goat anti-mouse IgG Fc (dianova, 115-136-071, dilution 1:100) for 45 min on ice followed by two washing steps. The APC signal median of alive single cells was acquired on a MACSQuant flow cytometer with lasers set to FSC: 430 V, SSC: 430 V and Y3 (APC): 660 V using MACSQuantify software (version 2.11). All measurements were performed in duplicates. Flowing Software (version 2.5.1, Turku Bioscience) was used for displaying histograms.

Whole mount immunofluorescent staining

All procedures involving zebrafish were performed according to EU guidelines and German legislation (EU Directive 2010_63, license AZ 325.1.53/56.1-TU-BS). Transgenic zebrafish (*D. rerio*) larvae at 2 dpf (days post fertilization) were anesthetized in 0.05% tricaine solution (Sigma, Steinheim, DE) for 20 min on ice. Afterwards, to achieve tissue fixation and permeabilization, the larvae were incubated with 4% formaldehyde plus 0.1% Triton X-100 in PBS for 3 h at 4 °C. During each incubation and washing step the samples were rotated to allow appropriate mixing of the solution. After fixation, the tissue was rinsed 10 min with PBS plus 0.1% Triton X-100 (TPBS) and subsequently incubated 15 min at −20 °C in ultrapure acetone without rotation. Samples were washed for 10 min in TPBS supplemented with 1% BSA and 1% DMSO (TPBS-BD). Tissue was blocked in TPBS-BD solution containing 5% goat serum (Vector labs/BIOZOL, Eching, DE) for 1 h at RT. Myc1-9E10 or mouse Hyper-Myc were diluted at a concentration of 0.1 µg/mL in TPBS-BD and incubated overnight at 4 °C. The morning after, samples were washed four times 10 min each in TPBS. Subsequently, samples were incubated with secondary goat *α*-mouse IgG (H+L) Alexa Fluor 488 antibody (Thermo Scientific, A11001; 1:300) diluted in TPBS-BD for 3 h at RT. Washing of the antibody solution was repeated as previously described. After staining, larvae were mounted in 1.2% ultra-low melting agarose and imaged with a confocal laser scanning microscope Zeiss Airyscan LSM 880 (Carl Zeiss Meditec AG, Jena, Germany) equipped with a dry 10× objective. Multiple z-Stacks were acquired throughout the whole larva. All images were processed for brightness and contrast using Zen Black Zeiss software (Carl Zeiss Meditec AG, Jena, Germany) and Inkscape photo editor (http://www.

inkscape.org/). Image acquisition and image processing were performed using identical parameters for all antibody stainings.

Stability assessment

IgG versions of Hyper-Myc were stored for 7 months at 4 °C in PBS without any stabilizer or protectant at a concentration ≥1 mg/mL. Aliquots of the same samples were stored at −80 °C and freshly thawed for the assay as reference, and protein concentration was determined again at the day of the assay to exclude that protein degradation occurred during the storage. In brief, 100 ng per well of a myc-peptide labelled unrelated protein (C-terminal tag fusion) was coated overnight at 4 °C in High binding 96 well plates (Corning, New York, USA). Afterwards, each well was blocked 1 h at RT with 350 µL MPBS-T and successively washed 3 times in PBS-T. Soluble IgG antibodies diluted in 100 µL MPBS-T at a concentration spanning from 1.28 pM to 60 nM were incubated in the antigen-coated wells for 1 h at 37 °C. The plates were washed 3 times with PBS-T. Species-specific secondary detection antibodies conjugated to HRP were diluted in MPBS-T and incubated for 1 h at 37 °C (goat anti-mouse A0168, Sigma, 1:42′000; goat anti-human A0170, Sigma, 1:42′000; donkey anti-rabbit 711-035-152, Jackson ImmunoResearch, 1:40′000). Unbound antibodies were removed by additional washing steps. Bound antibodies were detected with TMB substrate as previously described. Fresh and 7 months stored samples were tested in the same MTP for best comparability.

Acknowledgments: We are grateful to Herman Wätzig and Udo Burger for their help with the WES analysis, Toni Kirmann for the SEC measurements, Eric Dyrcz for analysis of array data and Daniela Rambow and Jürgen Kretschmer for technical assistance. We thank Reinhard Köster for the mScarlet-myc zebrafish transgenic line, Ulrike Theisen for the confocal microscope technical assistance and Timo Fritsch for excellent animal care.

Author contribution: All the authors have accepted responsibility for the entire content of this submitted manuscript and approved submission.

Research funding: G.R. and E.V.W. were supported by the EXIST Forschungstransfer grant 03EFLNI069 of the German Federal Ministry of Economic Affairs and Climate Action and the European Social Fund.

Conflict of interest statement: Three Hyper-Myc variants are made available to the research community through Abcalis GmbH. G.R., E.V.W. and S.D. are co-founders of Abcalis GmbH. R.B. and V.S. are co-founders of Pepperprint GmbH.

References

Baker, M. (2015). Reproducibility crisis: blame it on the antibodies. Nature 521: 274–276.

Berglund, L., Björling, E., Oksvold, P., Fagerberg, L., Asplund, A., Szigyarto, C.A.-K., Persson, A., Ottosson, J., Wernérus, H., Nilsson, P., et al. (2008). A genecentric Human Protein Atlas for expression profiles based on antibodies. Mol. Cell. Proteomics MCP 7: 2019–2027.

Bradbury, A. and Plückthun, A. (2015). Reproducibility: standardize antibodies used in research. Nature 518: 27–29.

Bradbury, A.R.M., Trinklein, N.D., Thie, H., Wilkinson, I.C., Tandon, A.K., Anderson, S., Bladen, C.L., Jones, B., Aldred, S.F., Bestagno, M., et al. (2018). When monoclonal antibodies are not monospecific: hybridomas frequently express additional functional variable regions. MAbs 10: 539–546.

Dimitrov, J.D., Kaveri, S.V., and Lacroix-Desmazes, S. (2014). Thermodynamic stability contributes to immunoglobulin specificity. Trends Biochem. Sci. 39: 221–226.

Dübel, S., Breitling, F., Fuchs, P., Braunagel, M., Klewinghaus, I., and Little, M. (1993). A family of vectors for surface display and production of antibodies. Gene 128: 97–101.

Evan, G.I., Lewis, G.K., Ramsay, G., and Bishop, J.M. (1985). Isolation of monoclonal antibodies specific for human c-myc proto-oncogene product. Mol. Cell Biol. 5: 3610–3616.

Frenzel, A., Kügler, J., Helmsing, S., Meier, D., Schirrmann, T., Hust, M., and Dübel, S. (2017). Designing human antibodies by phage display. Transfus. Med. Hemotherapy 44: 312–318.

Fuchs, P., Breitling, F., Little, M., and Dübel, S. (1997). Primary structure and functional scFv antibody expression of an antibody against the human protooncogen c-myc. Hybridoma 16: 227–233.

Fujiwara, K., Poikonen, K., Aleman, L., Valtavaara, M., Saksela, K., and Mayer, B.J. (2002). A single-chain antibody/epitope system for functional analysis of protein-protein interactions. Biochemistry 41: 12729–12738.

Gloor, S., Pongs, O., and Schmalzing, G. (1995). A vector for the synthesis of cRNAs encoding Myc epitope-tagged proteins in *Xenopus laevis* oocytes. Gene 160: 213–217.

Goodman, S.L. (2018). The antibody horror show: an introductory guide for the perplexed. New Biotechnol. 45: 9–13.

Gray, A.C., Bradbury, A.R.M., Knappik, A., Plückthun, A., Borrebaeck, C.A.K., and Dübel, S. (2020). Animal-derived-antibody generation faces strict reform in accordance with European Union policy on animal use. Nat. Methods 17: 755–756.

Halder, M., Barroso, J., and Whelan, M. (2020). EURL ECVAM recommendation on non-animal-derived antibodies, EUR 30185 EN. Publications Office of the European Union, Luxembourg, pp. 12–70.

Hilpert, K., Hansen, G., Wessner, H., Küttner, G., Welfle, K., Seifert, M., and Höhne, W. (2001). Anti-c-myc antibody 9E10: epitope key positions and variability characterized using peptide spot synthesis on cellulose. Protein Eng. 14: 803–806.

Jäger, V., Büssow, K., Wagner, A., Weber, S., Hust, M., Frenzel, A., and Schirrmann, T. (2013). High level transient production of recombinant antibodies and antibody fusion proteins in HEK293 cells. BMC Biotechnol. 13: 52.

Jarvik, J.W. and Telmer, C.A. (1998). Epitope tagging. Annu. Rev. Genet. 32: 601–618.

Kleymann, G., Ostermeier, C., Heitmann, K., Haase, W., and Michel, H. (1995). Use of antibody fragments (Fv) in immunocytochery. J. Histochem. Cytochem. 43: 607–614.

Krauss, N., Wessner, H., Welfle, K., Welfle, H., Scholz, C., Seifert, M., Zubow, K., Aÿ, J., Hahn, M., Scheerer, P., et al. (2008). The structure of the anti-c-myc antibody 9E10 Fab fragment/epitope

peptide complex reveals a novel binding mode dominated by the heavy chain hypervariable loops. Proteins 73: 552–565.

Kügler, J., Wilke, S., Meier, D., Tomszak, F., Frenzel, A., Schirrmann, T., Dübel, S., Garritsen, H., Hock, B., Toleikis, L., et al. (2015). Generation and analysis of the improved human HAL9/10 antibody phage display libraries. BMC Biotechnol. 15: 10.

Mollova, S., Retter, I., Hust, M., Dübel, S., and Müller, W. (2010). Analysis of single chain antibody sequences using the VBASE2 Fab analysis tool. In: Kontermann, R., and Dübel, S. (Eds.), *Antibody engineering*. Berlin, Heidelberg: Springer Protocols Handbooks, pp. 3–10.

Moutel, S., El Marjou, A., Vielemeyer, O., Nizak, C., Benaroch, P., Dübel, S., and Perez, F. (2009). A multi-Fc-species system for recombinant antibody production. BMC Biotechnol. 9: 14.

Ng, G.Y., George, S.R., Zastawny, R.L., Caron, M., Bouvier, M., Dennis, M., and O'Dowd, B.F. (1993). Human serotonin1B receptor expression in Sf9 cells: phosphorylation, palmitoylation, and adenylyl cyclase inhibition. Biochemistry 32: 11727–11733.

Rondot, S., Koch, J., Breitling, F., and Dübel, S. (2001). A helper phage to improve single-chain antibody presentation in phage display. Nat. Biotechnol. 19: 75–78.

Russo, G., Meier, D., Helmsing, S., Wenzel, E., Oberle, F., Frenzel, A., and Hust, M. (2018a). Parallelized antibody selection in microtiter plates. Methods Mol. Biol. 1701: 273–284.

Russo, G., Theisen, U., Fahr, W., Helmsing, S., Hust, M., Köster, R.W., and Dübel, S. (2018b). Sequence defined antibodies improve the detection of cadherin 2 (N-cadherin) during zebrafish development. New Biotechnol. 45: 98–112.

Schiweck, W., Buxbaum, B., Schätzlein, C., Neiss, H.G., and Skerra, A. (1997). Sequence analysis and bacterial production of the anti-c-myc antibody 9E10: the V(H) domain has an extended CDR-H3 and exhibits unusual solubility. FEBS Lett. 414: 33–38.

Schmidt, T.G. and Skerra, A. (1993). The random peptide library-assisted engineering of a C-terminal affinity peptide, useful for the detection and purification of a functional Ig Fv fragment. Protein Eng. 6: 109–122.

Schüchner, S., Behm, C., Mudrak, I., and Ogris, E. (2020). The Myc tag monoclonal antibody 9E10 displays highly variable epitope recognition dependent on neighboring sequence context. Sci. Signal. 13:eaax9730.

Shanbaky, N.M. and Pressley, T.A. (1994). Mammalian alpha 1-subunit of Na^+-K^+-ATPase does not need its amino terminus to maintain cell viability. Am. J. Physiol. 267: C590–C597.

Soltes, G., Hust, M., Ng, K.K.Y., Bansal, A., Field, J., Stewart, D.I.H., Dübel, S., Cha, S., and Wiersma, E.J. (2007). On the influence of vector design on antibody phage display. J. Biotechnol. 127: 626–637.

Stadler, V., Felgenhauer, T., Beyer, M., Fernandez, S., Leibe, K., Güttler, S., Gröning, M., König, K., Torralba, G., Hausmann, M., et al. (2008). Combinatorial synthesis of peptide arrays with a laser printer. Angew. Chem. Int. Ed. 47: 7132–7135.

Steinwand, M., Droste, P., Frenzel, A., Hust, M., Dübel, S., and Schirrmann, T. (2014). The influence of antibody fragment format on phage display based affinity maturation of IgG. MAbs 6: 204–218.

Stemmer, W.P. (1994). Rapid evolution of a protein *in vitro* by DNA shuffling. Nature 370: 389–391.

Taussig, M.J., Fonseca, C., and Trimmer, J.S. (2018). Antibody validation: a view from the mountains. New Biotechnol 45: 1–8.

TerBush, D.R. and Novick, P. (1995). Sec6, Sec8, and Sec15 are components of a multisubunit complex which localizes to small bud tips in *Saccharomyces cerevisiae*. J. Cell Biol. 130: 299–312.

Vita, R., Mahajan, S., Overton, J.A., Dhanda, S.K., Martini, S., Cantrell, J.R., Wheeler, D.K., Sette, A., and Peters, B. (2019). The Immune epitope database (IEDB): 2018 update. Nucleic Acids Res. 47: D339–D343.

Wang, W. and Roberts, C.J. (2013). Non-Arrhenius protein aggregation. AAPS J. 15: 840–851.

Ward, E.S., Güssow, D., Griffiths, A.D., Jones, P.T., and Winter, G. (1989). Binding activities of a repertoire of single immunoglobulin variable domains secreted from *Escherichia coli*. Nature 341: 544–546.

Wong, T.S., Roccatano, D., Zacharias, M., and Schwaneberg, U. (2006). A statistical analysis of random mutagenesis methods used for directed protein evolution. J. Mol. Biol. 355: 858–871.

Supplementary Material: The online version of this article offers supplementary material (https://doi.org/10.1515/hsz-2021-0405).